JOURNAL OF AGRICULTURAL AND FOOD CHEMISTRY

pubs.acs.org/JAFC Article

Acetylation and Phosphorylation Regulate the Role of Pyruvate Kinase as a Glycolytic Enzyme or a Protein Kinase in Lamb

Chi Ren, Xin Li, Juan Li, Xiaolan Huang, Yuqiang Bai, Martine Schroyen, Chengli Hou, Zhenyu Wang, and Dequan Zhang*

Cite This: *J. Agric. Food Chem.* 2024, 72, 11724−11732 Read Online

ACCESS | Metrics & More | Article Recommendations | Supporting Information

ABSTRACT: Protein post-translational modifications (PTMs) play an essential role in meat quality development. However, the effect of specific PTM sites on meat proteins has not been investigated yet. The characteristics of pyruvate kinase M (PKM) were found to exhibit a close correlation with final meat quality, and thus, serine 99 (S99) and lysine 137 (K137) in PKM were mutated to study their effect on PKM function. The structural and functional properties of five lamb PKM variants, including wild-type PKM (wtPKM), PKM_S99D (S99 phosphorylation), PKM_S99A (PKM S99 dephosphorylation), PKM_K137Q (PKM K137 acetylation), and PKM_K137R (PKM K137 deacetylation), were evaluated. The results showed that the secondary structure, tertiary structure, and polymer formation were affected among different PKM variants. In addition, the glycolytic activity of PKM_K137Q was decreased because of its weakened binding with phosphoenolpyruvate. In the PKM_K137R variant, the actin phosphorylation level exhibited a decrease, suggesting a low kinase activity of PKM_K137R. The results of molecular simulation showed a 42% reduction in the interface area between PKM_K137R and actin, in contrast to wtPKM and actin. These findings are significant for revealing the mechanism of how PTMs regulate PKM function and provide a theoretical foundation for the development of precise meat quality preservation technology.

KEYWORDS: *pyruvate kinase, protein phosphorylation, protein acetylation, bifunctional enzyme*

INTRODUCTION

Pyruvate kinase (PK) is an important glycolytic rate-limiting enzyme, which catalyzes the step from phosphoenolpyruvate (PEP) to pyruvate and generates adenosine 5′-triphosphate (ATP). It has been proven that the isoform of PK in post-mortem muscle (PKM) is closely linked to meat quality through glycolysis regulation. Pale, soft, and exudative (PSE) meat caused by fast glycolysis leads to economic loss and food waste, which cannot be ignored. A previous study showed that the Michaelis−Menten constant of PKM isolated from PSE meat is 5 times lower than that isolated from normal meat, suggesting a higher activity of PKM in PSE meat.[1] Through adding a PKM inhibit or activator to post-mortem muscle, it was observed that PKM affected glycolysis, pH value, protein degradation, and μ-calpain activity.[2] A proteomics study found a decreasing expression of PKM during the post-mortem stage linked to low beef tenderness.[3] PKM is identified as a powerful predictor for lamb,[4] beef,[5] and pork[6] meat quality like tenderness, color, and water holding capacity. Besides the well-known role of PKM as a glycolytic enzyme, it also moonlights as a protein kinase upon phosphorylation by transferring the phosphoryl group from PEP to a protein substrate.[7] PKM is a multifunctional enzyme that widely regulates various biochemical activities.

The structure and function of proteins are regulated by protein post-translational modifications (PTMs). Many studies have noted that PTMs impact protein activity, stability, and structure, thus playing important roles in maintaining diverse functions.[8] Protein phosphorylation and acetylation are two common PTMs, occurring in serine (S), threonine (T), tyrosine (Y), and lysine (K) residues, respectively. The binding between PKM and fructose 1,6-bisphosphate (FBP) is restrained when PKM is acetylated at K433, inhibiting PKM activity.[9] Y105 phosphorylation of PKM disrupts its tetramer formation and this also inhibited PKM activity.[10] Besides, the PTMs status has a vital effect on muscle proteins and consequently affects meat quality development.[11] The phosphorylation and acetylation of PKM in post-mortem meat have gradually obtained attention because of their importance for meat quality. The phosphorylation and acetylation sites of PKM have been widely documented with regard to changes in various factors such as glycolytic rates in lamb,[12] color stability in lamb,[13] post-mortem time in pork,[14] and others. Certain PTMs sites were speculated to be important in shaping PKM properties and thus affect meat quality. However, the potential impact of these specific phosphorylated and acetylated sites on the PKM characteristics concerning meat quality requires additional investigation.

The *Escherichia coli* recombinant expression system and site-directed mutagenesis are common technologies in the field of molecular biology for examining the effect of specific sites on

Received: January 4, 2024
Revised: April 22, 2024
Accepted: April 26, 2024
Published: May 8, 2024

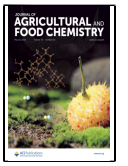

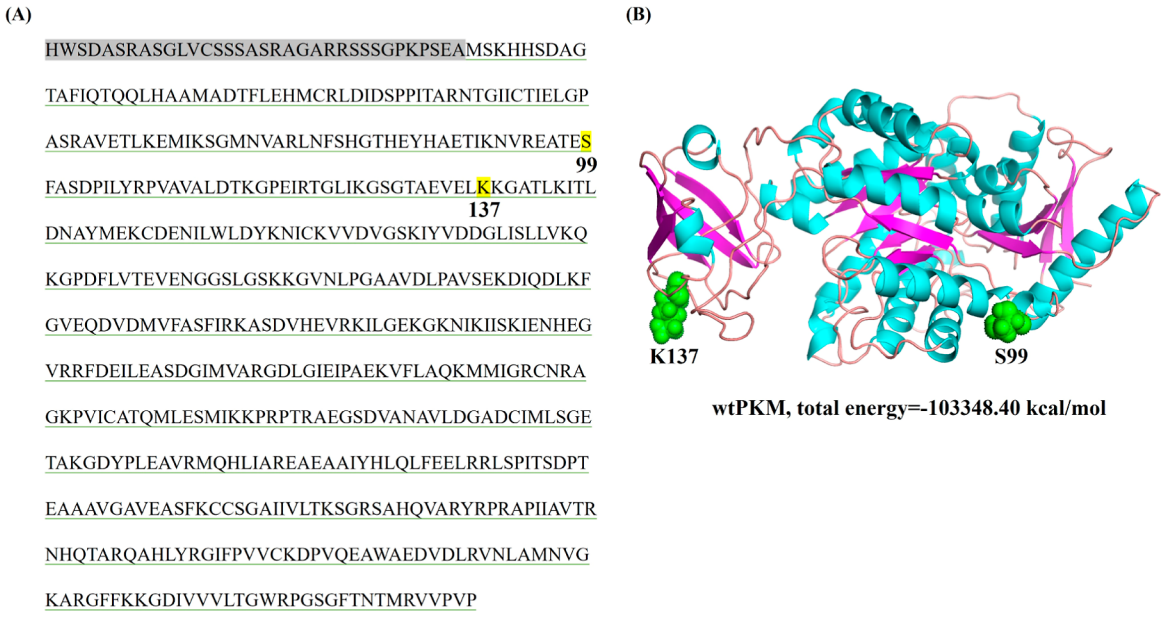

Figure 1. Basic information on lamb PKM. (A) Sequence of lamb PKM. The sequences with gray color were cut off when overexpressed and purified. The specific sites with yellow color were practically mutated in the *E. coli* recombinant expression system. (B) 3D structure of lamb PKM after molecular dynamics simulation. PKM S99 was located in the A domain and PKM K137 was located in the B domain.

protein function, although they are not extensively used in the field of meat science. In the present study, specific phosphorylated and acetylated sites of PKM were mutated using these technologies, and the effect of these mutations on PKM activity, structure, and function was evaluated. This research broadens the insights into the possible regulation of PTMs on PKM in post-mortem meat.

MATERIALS AND METHODS

Protein Overexpression and Purification. The sequence of lamb PKM was obtained from the public database of UniProt (ID: W5QC41). Lamb PKM has a disordered sequence of 34 amino acids at the N-terminal that reduces protein stability and solubility (Figure S1A). PKM sequence alignment by CLUSTALW of different species showed that these 34 amino acids were only present in lamb (Figure S1B). In order to improve PKM expression and stability, the first 34 amino acids were cut off before plasmid construction. The detailed sequence of PKM is shown in Figure 1A. The wild-type PKM (wtPKM) gene was cloned into a pET-32a vector with the maltose binding protein (MBP) label. The constructed vector acted as a template to produce the mutated PKM variants. The wtPKM and mutated PKM were overexpressed and purified using the *E. coli* recombinant expression system and site-directed mutagenesis.[15] Briefly, the constructed vector of wtPKM acted as the template to produce PKM S99D, S99A, K137Q, and K137R by site-directed mutagenesis, and then DNA sequence technology was used to detect the mutation (Figure S2). All of the different vectors were transformed into *E. coli* BL21 (DE3) (Solarbio Life Science, Beijing, China). A single colony was inoculated on Luria−Bertani media with ampicillin and incubated at 37 °C until an OD_{600} of 0.8. Isopropyl β-D-1-thiogalactopyranoside (IPTG) was added to the cultures with a final concentration of 0.2 mM. The cultures were grown at 16 °C overnight and then harvested through centrifugation. The sediment was resuspended with 30 mL of buffer A (50 mM Tris, pH 8.0, 300 mM NaCl, 10 mM imidazole) and disrupted by high pressure. After centrifugation, the supernatant was incubated with Ni-beads, and the targeted protein was eluted by buffer B (50 mM Tris, pH 8.0, 300 mM NaCl, 1 M imidazole). Size exclusion chromatography Superdex 200 16/60 column (GE, Boston MA, USA) was applied to obtain purified PKM variants (Figure S3).

PKM Glycolytic Activity. The glycolytic activity of wtPKM and mutated PKMs was measured by a commercial kit (Solarbio Life Science). The samples were prepared following the manufacturer's protocol. The absorbance differences from 20 s to 5 min 20 s at 340 nm were detected to evaluate PKM activity.

PKM Kinase Assay on Phosphorylating Actin. The previous study showed that actin was one of the phosphorylated substrates of PKM, therefore the kinase assay on actin was performed to evaluate PKM kinase activity.[16] The wtPKM and mutated PKMs were incubated with actin (Shanghai Yuanye Bio-Technology Co., Ltd., Shanghai, China) at 37 °C for 0.5 and 6 h in a buffer consisting of 100 mM KCl, 50 mM $MgCl_2$, 1 mM DTT, 1 mM $NaVO_4$, 5% glycerin, 2 mM PEP, 30 mM HEPES, pH 7.5. The concentration of wtPKM and mutated PKMs was 0.4 μg/μL, and the concentration of actin was 0.2 μg/μL. A sample only including actin was regarded as a negative control (Figure S4). Zn^{2+}-Phos-tag SDS-PAGE (Wako, Osaka, Japan) was performed to measure the phosphorylation level of actin. A Western blot was carried out to detect actin. The primary antibody of actin (1:1000 dilution, A1011, ABclonal) was incubated at 4 °C overnight, and the secondary antibody (1:1000 dilution, AS014, ABclonal) was incubated at room temperature for 2 h.

Secondary Structure. The secondary structure was detected using a Fourier transform infrared spectrometer (Bruker Co., Ltd., Ettlingen, Germany) with a resolution of 8 cm^{-1}, a scan number of 64, and a scan range of 4000−600 cm^{-1}. The spectroscopic data was processed by an OMINC instrument, and the secondary structure was analyzed by a Peakfit instrument (Systat Software Inc., San Jose, CA).

Intrinsic Fluorescence. The intrinsic fluorescence of wtPKM and mutated PKMs was detected using a F-380 fluorescence-spectrophotometer (Tianjin Gangdong Sci. &Tech. Co., Ltd., Tianjin, China) according to the method of Li et al. with minor modifications.[17] The PKMs (0.05 mg/mL) were dissolved in 0.6 M NaCl (pH 6.25) to measure their intrinsic fluorescence. The excitation wavelength was 295 nm, and the emission wavelength was collected at 300−400 nm with 10 nm slits and 240 nm/min scan rate.

Thioflavin-T (ThT) Fluorescence. The aggregates of PKM were monitored by ThT fluorescence according to the method of Guerrero-Mendiola et al.[18] Two hundred micrograms of wtPKM and mutated PKMs was added into the buffer of 25 mM Tris-HCl, pH 7.6, 100 mM $(CH_3)_4NCl$, 10 mM DTT, and incubated at 60 °C for 1.5 h. Then, 10 μM ThT was added to the incubated samples for detection. The excitation wavelength was 445 nm, and the emission

https://doi.org/10.1021/acs.jafc.4c00082
J. Agric. Food Chem. 2024, 72, 11724−11732

Table 1. Differences of Total Energy between PKM Phosphorylation Mutation and Dephosphorylation Mutation by Using Molecular Dynamics Simulation

phosphorylation mutation	total energy (kcal/mol)[a]	dephosphorylation mutation	total energy (kcal/mol)[b]	difference[c]
S37D	−102,938	S37A	−103,330	392
S79D	−103,300	S79A	−103,273	27
S99D	−103,704	S99A	−102,867	836
S102D	−103,544	S102A	−102,993	551
S129D	−103,153	S129A	−103,357	204
S204D	−103,123	S204A	−103,010	113
S224D	−103,191	S224A	−102,789	402
S251D	−103,526	S251A	−103,217	309
S364D	−103,341	S364A	−103,427	85
S521D	−103,260	S521A	−103,292	33
T41D	−103,016	T41A	−103,580	565
T82D	−103,651	T82A	−103,468	182
T131D	−103,713	T131A	−103,446	267
T330D	−102,730	T330A	−102,902	171
Y85E	−103,207	Y85F	−103,467	260
Y150E	−102,801	Y150F	−102,803	2
Y372E	−103,681	Y372F	−103,333	348

[a]The total energy of phosphorylation mutation. [b]The total energy of dephosphorylation mutation. [c]The absolute value of total energy difference between phosphorylation mutation and dephosphorylation mutation.

wavelength was collected at 460−600 nm with 10 nm slits and 1200 nm/min scan rate.

MOLECULAR SIMULATION

Molecular Dynamics Simulation after Site Mutation. The 3D structures of wtPKM were constructed using BIOVIA Discovery Studio 2019 (Dassault Systemes BIOVIA Ltd., France). Seventeen phosphorylated and 17 acetylated sites of lamb PKM (Table S1, unpublished data with identifier PXD046140 uploaded to ProteomeXchange) were mutated following the principle of charge property according to previous studies.[19−21] Serine (S) and threonine (T) were mutated to aspartic acid (D) to simulate phosphorylation and to alanine (A) to simulate dephosphorylation. Tyrosine (Y) was mutated to glutamic acid (E) to simulate phosphorylation and to phenylalanine (F) to simulate dephosphorylation. Lysine (K) was mutated to glutamine (Q) to simulate acetylation and to arginine (R) to simulate deacetylation. The process of molecular dynamics simulation was performed to calculate the total energy of wtPKM and mutated PKMs in order to screen overexpressed sites in the *E. coli* recombinant expression system.

PKM Docked to PEP and Adenosine Diphosphate (ADP). The 2D structures of PEP (PubChem CID: 1005) and ADP (PubChem CID: 6022) were obtained from the public database of PubChem. The 3D structures of wtPKM and mutated PKMs were adopted after molecular dynamics simulation. They were imported to Schrödinger Maestro v13.5 for the processing of Protein Preparation and Refinement and LigPrep. The wtPKM and mutated PKMs were docked to PEP and ADP, respectively, in the Glide module. G score was used to evaluate the docking results. The 3D interaction pattern of PKM with PEP and ADP was analyzed in PyMOL 2.5.4, and the 2D interaction pattern of PKM with PEP and ADP was analyzed in BIOVIA Discovery Studio 2019.

PKM Docked to Actin. The amino acid sequence of lamb actin was obtained from the public database of UniProt (ID: W5NYJ1), and its 3D structure was constructed in BIOVIA Discovery Studio 2019. The online website of GRAMM Docking (https://gramm.compbio.ku.edu/request) was used to process PKM and actin docking. Actin was set as a ligand, and wtPKM and the mutated PKM_K137R were set as receptors. The receptor interface residue was thus K137 of wtPKM or R137 of the mutated PKM. The best conformation of PKM−actin was optimized in Schrödinger Maestro v13.5. The online website of PDBePISA (https://www.ebi.ac.uk/pdbe/pisa/) was used to calculated the interface area between PKM and actin. The 3D interaction pattern of PKM and ADP was analyzed in PyMOL 2.5.4.

Statistical Analysis. The results of PKM activity and the actin phosphorylation level were recorded as mean values ± standard error. Duncan's test of ANOVA and *t*-test were used to analyze significant differences among samples ($P < 0.05$) in SPSS Statistic 22.0 (SPSS Inc., Chicago, IL, USA). The band intensity of phosphorylated and dephosphorylated actin was analyzed by Quantity-One 4.6.2 (Bio-Rad).

RESULTS

Changes of Total Energy after PKM Mutation. Some phosphorylation and acetylation sites of PKM were mutated, after which a molecular dynamics simulation was performed using the Discovery Studio software. The total energy of wtPKM was −103,348.40 kcal/mol (Figure 1B). The difference in total energy between PKM_S99D and PKM_S99A was the largest compared with other phosphorylation mutation comparisons (Table 1). The total energy of PKM_S99D was higher than that of wtPKM, but the total energy of PKM_S99A was lower than that of wtPKM, which suggested a possible stable structure of PKM_S99A. The difference of total energy between PKM_K137Q and PKM_K137R was largest compared with other acetylation mutation comparisons (Table 2). The total energy of PKM_K137Q was lower than that of wtPKM, showing a possible stable structure for K137 acetylation. Thus, the specific phosphorylation site of S99 and the specific acetylation site of K137 were selected as practical mutated sites according to the results of the total energy in the present study. PKM sequences of lamb, bovine, pig, human,

https://doi.org/10.1021/acs.jafc.4c00082
J. Agric. Food Chem. 2024, 72, 11724−11732

Table 2. Differences of Total Energy between PKM Acetylation Mutation and Acetylation Mutation by Using Molecular Dynamics Simulation

acetylation mutation	total energy (kcal/mol)[a]	deacetylation mutation	total energy (kcal/mol)[b]	difference[c]
K64Q	−102,989	K64R	−103,424	436
K68Q	−103,404	K68R	−103,162	242
K91Q	−103,113	K91R	−103,080	33
K117Q	−103,032	K117R	−103,228	196
K127Q	−103,357	K127R	−103,189	169
K137Q	−102,720	K137R	−103,637	918
K143Q	−102,842	K143R	−103,504	662
K164Q	−103,174	K164R	−103,534	360
K168Q	−103,078	K168R	−103,042	35
K208Q	−103,237	K208R	−103,256	18
K272Q	−103,656	K272R	−103,057	599
K307Q	−103,228	K307R	−103,493	265
K313Q	−103,067	K313R	−103,199	132
K338Q	−102,956	K338R	−103,149	193
K435Q	−103,486	K435R	−103,483	3
K500Q	−103,270	K500R	−103,150	119
K507Q	−103,296	K507R	−103,443	147

[a]The total energy of acetylation mutation. [b]The total energy of deacetylation mutation. [c]The absolute value of total energy difference between acetylation mutation and deacetylation mutation.

mouse, and rabbit were aligned by CLUSTALW. The result showed that S99 and K137 were two conserved sites of PKM (Figure S5), suggesting that the mutation of these two sites might play an important role in PKM function.

Effect of Phosphorylation and Acetylation on the Glycolytic Activity of PKM. The glycolytic activity of the different PKM variants was evaluated. The results showed that PKM_K137Q had the lowest glycolytic activity compared with the others tested ($P < 0.05$, Figure 2A), but there were no significant differences between wtPKM, PKM_S99D, PKM_S99A, and PKM_K137R ($P > 0.05$, Figure 2A). This suggested that the glycolytic activity of PKM was greatly decreased when the K137 site was acetylated. PEP and ADP are two substrates of PKM in glycolysis. The binding capacity between PKM variants with PEP and ADP was evaluated through molecular docking in order to reveal a possible mechanism. The G score represents the binding capacity between the complexes. The higher the absolute value of the G score, the better the binding capacity. The G score of PKM_K137Q and PEP was −3.921 kcal/mol, which was 10% less than the G score of wtPKM and PEP (Figure 2B,C). The results of the 2D interaction pattern showed that more interaction existed between wtPKM and PEP. In addition, the binding capacity between the different PKM variants and ADP was also evaluated. The G score of wtPKM and ADP was −5.439 kcal/mol, and the G score of PKM_K137Q and ADP was −5.461 kcal/mol (Figure 3A,B). The G score of the PKM variants with ADP was higher than that of the PKM variants with PEP, which indicated that the affinity of ADP was stronger for PKM. However, only a 0.4% difference was calculated between the G scores of wtPKM-ADP and PKM_K137Q-ADP.

Effect of Phosphorylation and Acetylation on PKM as a Protein Kinase. The PKM variants were incubated with actin to investigate the activity of PKM as a protein kinase. The actin phosphorylation level of the different PKM variants was insignificantly different at 0.5 h of incubation ($P > 0.05$, Figure 4A). When incubating for 6 h, the actin phosphorylation level of wtPKM and PKM_S99D significantly increased ($P < 0.05$, Figure 4A). Compared with 0.5 h, although the actin phosphorylation level also increased for PKM_S99A and PKM_K137Q at 6 h, there was no significant difference ($P > 0.05$, Figure 4A). The results showed a significant decrease of kinase activity of PKM_S99A, K137Q, and K137R at 6 h compared with that of wtPKM. The actin phosphorylation level of PKM_K137R was lowest among them, suggesting the most significant change induced by K137 deacetylation. The docking of wtPKM and PKM_K137R with actin was performed respectively. The binding energy of PKM_K137R and actin was −564 kJ/mol, which was reduced 2% compared

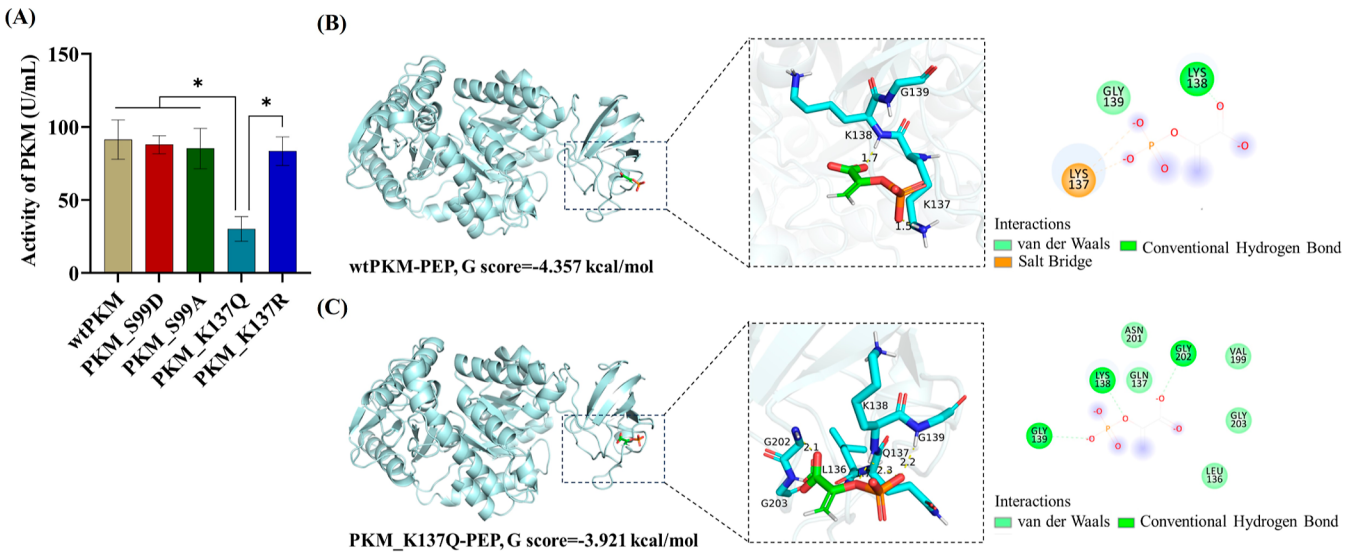

Figure 2. Glycolytic activity of PKM variants and simulative docking between PKM variants and PEP. (A) Detection of glycolytic activity of PKM variants by using a commercial kit. (B) Simulative docking between wtPKM and PEP. (C) Simulative docking between PKM_K137Q and PEP. The G score was calculated to evaluate the binding energy of PKM variants and PEP. 2D and 3D interaction patterns showed the detailed information between their binding. *$P < 0.05$.

https://doi.org/10.1021/acs.jafc.4c00082
J. Agric. Food Chem. 2024, 72, 11724−11732

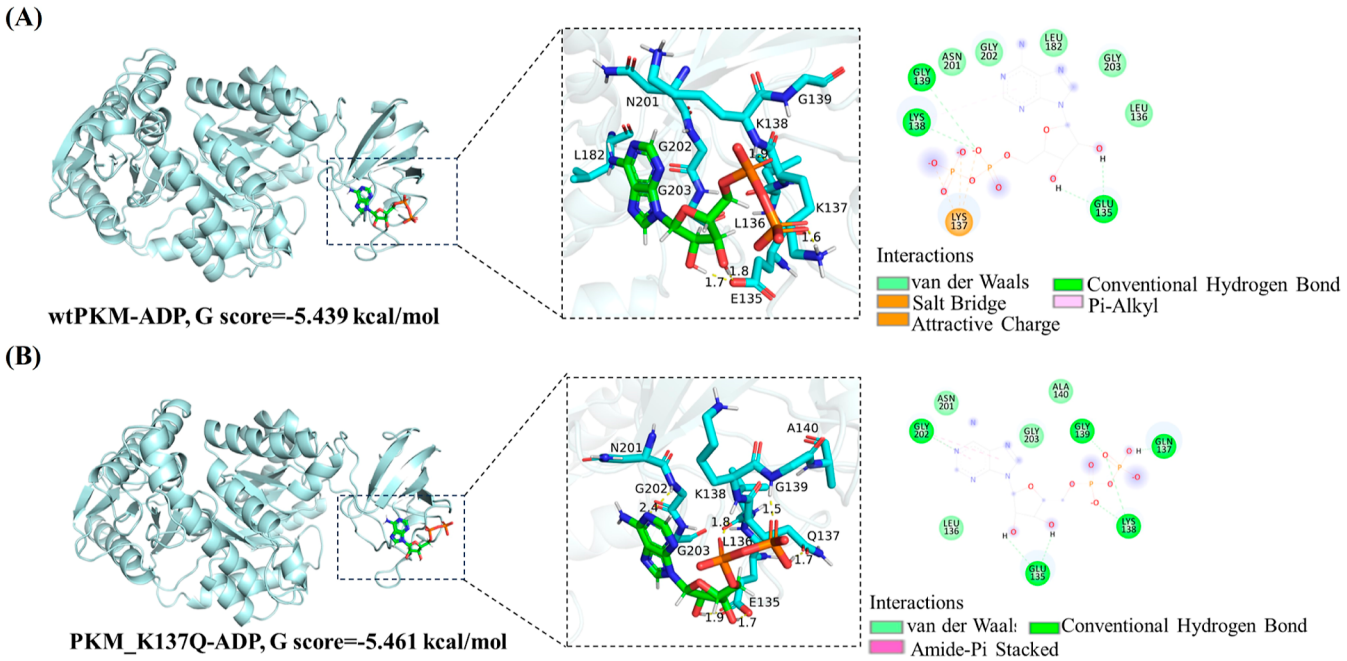

Figure 3. Simulative docking between PKM variants and ADP. (A) Simulative docking between wtPKM and ADP. (B) Simulative docking between PKM_K137Q and ADP. The G score was calculated to evaluate the binding energy of PKM variants and ADP. 2D and 3D interaction patterns showed the detailed information between their binding.

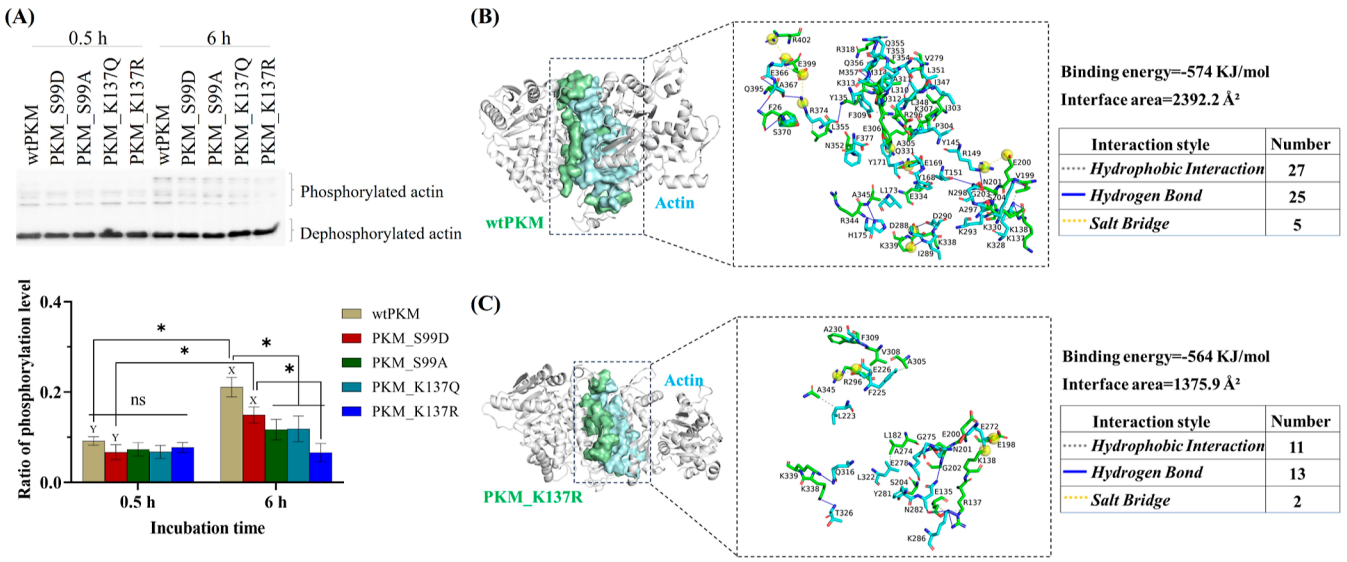

Figure 4. Kinase activity of PKM variants and simulative docking between PKM variants and actin. (A) Actin phosphorylation level catalyzed by PKM variants during 0.5 and 6 h incubation at 37 °C. (B) Simulative docking between wtPKM and actin. (C) Simulative docking between PKM_K137R and actin. 3D interaction patterns showed the detailed information between binding interfaces. *$P < 0.05$. ns $P > 0.05$.

with the binding energy of wtPKM and actin (Figure 4B,C). The interface area of PKM_K137R and actin was 1375.9 Å^2, which was 42% less compared with the interface area of wtPKM and actin (Figure 4B,C). The analysis of the interface between wtPKM and actin showed that there were 27 couples of hydrophobic interaction, 25 couples of hydrogen bonds, and 5 couples of salt bridges. However, the interaction of the interface between PKM_K137R and actin was declined to 11 couples of hydrophobic interaction, 13 couples of hydrogen bonds, and 2 couples of salt bridges.

Effect of Phosphorylation and Acetylation on the PKM Structure. The dephosphorylation of PKM S99 led to a decrease of random coils and α-helices compared with the other PKM variants (Figure 5A). The intrinsic fluorescence reflected the changes of protein tertiary structure. The dephosphorylation of PKM S99 and deacetylation of PKM K137 caused a decline of the intrinsic fluorescence intensity compared with the other PKM variants (Figure 5B), indicating lower exposure of chromogenic groups in PKM_S99A and PKM_K137R. Cryoelectron microscopy is a direct tool to analyze protein structure, but its sample pretreatment procedure is very strict. ThT fluorescence was used to represent the aggregate formation of proteins, and the monomeric protein does not cause obvious variation of ThT fluorescence.[22] Thus, the present study used ThT fluorescence to detect the aggregate formation of proteins. Compared with

https://doi.org/10.1021/acs.jafc.4c00082
J. Agric. Food Chem. 2024, 72, 11724−11732

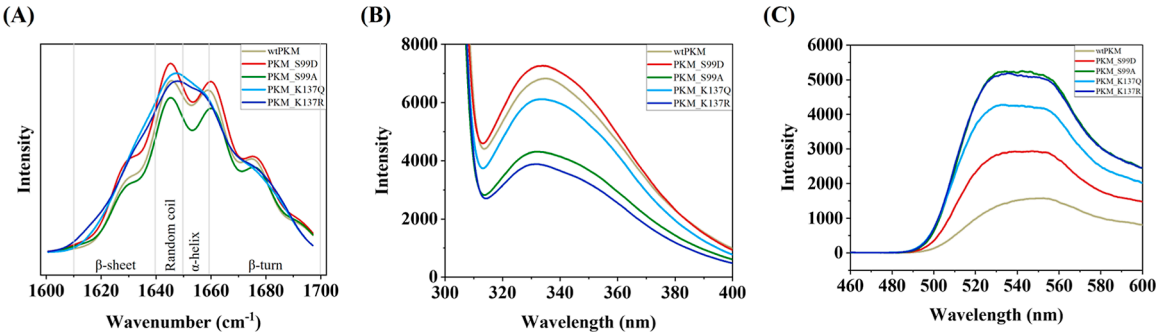

Figure 5. FT-IR spectra (A), intrinsic fluorescence spectra (B), and ThT fluorescence spectra (C) of PKM variants.

wtPKM, all mutations of PKM in the present study resulted in the increase of ThT fluorescence intensity (Figure 5C). The ThT fluorescence intensities of PKM_S99A and PKM_K137R were the most elevated among all PKM variants, which suggested that the dephosphorylation of PKM S99 and deacetylation of PKM K137 might cause more formation of PKM aggregation.

DISCUSSION

It is clear that PKM plays an important role in final meat quality as there is a significantly negative relationship between PKM gene expression and the final pH value in post-mortem meat.[23] The important role of PKM as a glycolytic enzyme in meat science has therefore been widely investigated. Recently, another function of PKM as a protein kinase is reported, resulting in the knowledge that PKM is a bifunctional protein.[24] When PKM acts as a glycolytic enzyme, it catalyzes PEP and ADP to generate pyruvate and ATP. However, PKM can also transfer the phosphate group from PEP to a protein substrate and act as a protein kinase.[25] PKM inhibits myofibrillar protein degradation by phosphorylation which will regulate meat tenderization.[16] There are more than 900 protein substrates of PKM,[26] suggesting a wide effect of PKM on phosphorylating proteins.

Although it has been proven that PTM regulates meat quality through PKM regulation and numerous PTM sites of PKM have been identified, the effect of specific PTM sites on PKM function has not been investigated yet. Molecular simulation is an emerging technology which has been widely applied to reasonably predict protein changes and visualize detailed information.[27] In this study, this simulation technology and practical experiments were combined to analyze the effect of PTM sites on the PKM function. Seventeen phosphorylation and acetylation sites of PKM in prerigor and postrigor lamb were mutated and analyzed using BIOVIA Discovery Studio, respectively. S99 and K137 of PKM were selected due to the large differences of total energy after molecular dynamics simulation (Tables 1 and 2). These two mutations were present on the conserved sites of lamb PKM that have never been reported before. Conserved sites control protein function, for example, human PKM_S37 and PKM_K305 have been revealed changing PKM function effectively.[15,28] The newly reported sites S99 and K137 being in conserved regions of PKM will thus probably provide more information about lamb PKM. Five PKM variants, including wtPKM, PKM_S99D, PKM_S99A, PKM_K137Q, and PKM_K137R, were overexpressed and purified through the *E. coli* recombinant expression system. The monomer of PKM has four domains. Taking PKM in rabbit muscle as an example, residues 1−42 present the N domain, 43−115 and 219−387 are the A domain, 116−218 form the B domain, and 388−530 are the C domain.[29] S99 and K137 of PKM were located in the A and B domains, respectively. Li et al. reported that changes in the B domain were more sensitive and important for PKM glycolytic activity because of its high flexibility.[30] In this study, PKM_K137Q showed a lower glycolytic activity compared with the other four PKM variants (Figure 2A). The results of molecular docking suggested that the binding of PKM_K137Q and PEP decreased, which might be a main reason for the low glycolytic activity of PKM_K137Q rather than the binding of PKM_K137Q and ADP. A previous study of molecular docking showed that K433 acetylation led to a steric hindrance of FBP binding to PKM via neutralization of the charge on the lysine side chain, which was similar to the result performed in the binding assay.[9] The phosphorylation and dephosphorylation mutations of PKM S99 did not show significant effects on PKM glycolytic activity in the present study. However, in another study, it was shown that PKM T105 phosphorylation caused reduced glycolytic activity.[31] Yet another study showed that the phosphorylation of PKM S287 resulted in increased glycolytic activity.[32] Thus, it is necessary to investigate the effect of specific PTM sites on PKM function in order to better understand the regulatory mechanism of PKM on meat quality development. More functional analysis on PKM S99 and K137 should be conducted, taking into account various meat samples for testing. Moreover, the specific inhibitor or activator of these important sites of PKM could be developed and applied in meat packaging or preservation in the future to regulate glycolysis and meat quality through changing PKM function.

The role of PKM as a protein kinase also takes part in many cellular activities through regulating cellular localization, protein−protein interaction, and so on.[33] In the present study, the assay of the actin phosphorylation level evaluated the capacity of PKM as a protein kinase. Actin phosphorylation levels of the variants PKM_S99A, K137Q, and K137R were significantly decreased at 6 h, suggesting a reduced kinase activity. The actin phosphorylation level catalyzed by PKM_K137R was reduced mostly among them (Figure 4A), showing that the activity of PKM as a protein kinase was maximally inhibited when its K137 was deacetylated. Thus, molecular docking was performed to analyze the possible reason behind this reduction. The results of GRAMM Docking, the lower binding energy, the interface area, and interaction of PKM_K137R with actin partly explained the reason for the low actin phosphorylation level of PKM_K137R. The deacetylation of PKM K137 inhibited the capacity of PKM as a protein kinase through changing PKM−actin interaction. It is therefore essential to reveal which

https://doi.org/10.1021/acs.jafc.4c00082
J. Agric. Food Chem. 2024, 72, 11724−11732

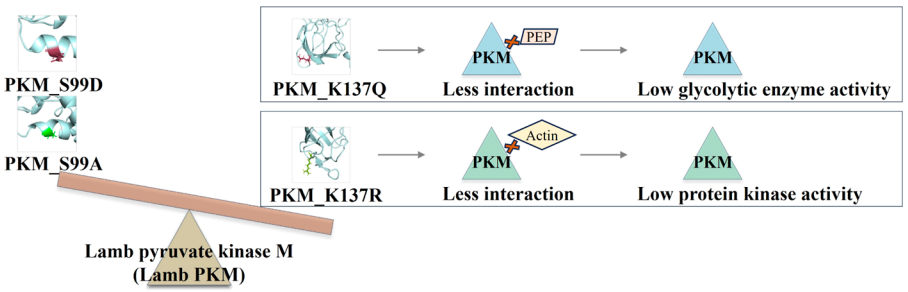

Figure 6. Schematic summary of the effect of the specific PTM site on PKM function. The interaction between PKM_K137Q and PEP was decreased, which led to a low glycolytic enzyme activity. The interaction between PKM_K137R and actin was decreased, which led to a low protein kinase activity. PKM_K137 was a more important site to regulate the PKM structure and function.

specific phosphorylation sites of actin were regulated by different PKM variants through phosphoproteomics in further studies to reveal the comprehensive regulation mechanism. In addition, the different polymers of PKM control its bifunctional characteristics. The PKM dimer is mainly responsible for protein kinase activity, and the tetramer is mainly responsible for glycolytic enzyme activity.[15] The fluorescence intensity of ThT reflects protein aggregation, but it will not show notable fluorescent changes with monomeric proteins. Although there were various differences between the PKM variants (Figure 5C), it was difficult to recognize PKM dimers or tetramers in the present study. However, it is still valuable to see that phosphorylation or acetylation has a visible effect on the formation of PKM oligomerization. Park et al. reported that PKM K305 acetylation restrained its glycolytic activity through prevention of the formation of a PKM tetramer.[34] PKM is a sarcoplasmic protein in post-mortem meat, but it will translocate to other places in some cases. For example, the acetylation of PKM K433 would result in PKM translocation to the nucleus,[9] but the phosphorylation of PKM S37 inhibited its nuclear translocation.[35] When cells underwent oxidative stress, PKM translocated to mitochondria and then phosphorylated Bcl2 to regulate apoptosis, which was important for reactive oxygen species adaptation of cells.[36]

PTM plays an important role in the changes of the PKM structure. When PKM K433 was mutated to PKM Q433 to simulate acetylation, the side chain of PKM Q433 showed the removal of the binding site with fructose 1,6-bisphosphate (FBP), which resulted in a decrease in PKM glycolytic activity.[15] When PKM K137 was mutated to PKM Q137 in the present study, the salt bridge between K137 and PEP was broken (Figure 2B,C), which might lessen the binding between PKM_K137Q and PEP and subsequently decline its glycolytic activity. The lowest intrinsic fluorescence intensity of PKM_K137R suggested a tighter tertiary structure compared with the other PKM variants (Figure 5B), which might hide more binding sites for actin, and this could thus be responsible for a lower actin phosphorylation level. Compared with the effect of phosphorylation and dephosphorylation on PKM S99, it was found that acetylation and deacetylation of PKM K137 had a greater effect on its function (Figure 6). PKM K137 is located in the B domain which is a very flexible area of the PKM monomer.[37] Thus, the PTM of this B domain might change the PKM function more easily. PKM K137 might affect the development of meat quality through the effect of its acetylation on glycolysis or its deacetylation on protein phosphorylation.

In summary, the effect of PKM phosphorylation and acetylation at S99 and K137 on PKM function was investigated through the *E. coli* recombinant expression system, site-directed mutagenesis, and molecular simulation. The acetylation and deacetylation of PKM K137 greatly impacted the PKM biofunction compared with PKM S99. The acetylation of PKM K137 inhibited its glycolytic activity possibly through the decrease of the binding with PEP. The deacetylation of PKM K137 might lessen its binding with actin and thus decrease PKM-induced actin phosphorylation. This study highlights the important effect of PTMs on PKM, and these sites can be regarded as important targets to develop meat quality preservation technology in the further study.

■ ASSOCIATED CONTENT

Supporting Information

The Supporting Information is available free of charge at https://pubs.acs.org/doi/10.1021/acs.jafc.4c00082.

Identified phosphorylation and acetylation sites of lamb PKM; PKM sequence analysis; DNA sequence of wtPKM and its mutated variants; images of recombinant PKM variants with the MBP label by Coomassie staining; kinase activity of PKM variants; and PKM sequence alignment of lamb, bovine, human, mouse, rabbit, and pig by CLUSTALW (PDF)

■ AUTHOR INFORMATION

Corresponding Author

Dequan Zhang − *Institute of Food Science and Technology, Chinese Academy of Agricultural Sciences/Key Laboratory of Agro-Products Quality & Safety in Harvest, Storage, Transportation, Management and Control, Ministry of Agriculture and Rural Affairs, Beijing 100193, P. R. China;* orcid.org/0000-0003-3277-6113; Email: dequan_zhang0118@126.com

Authors

Chi Ren − *Institute of Food Science and Technology, Chinese Academy of Agricultural Sciences/Key Laboratory of Agro-Products Quality & Safety in Harvest, Storage, Transportation, Management and Control, Ministry of Agriculture and Rural Affairs, Beijing 100193, P. R. China; Precision Livestock and Nutrition Unit, Gembloux Agro-Bio Tech, University of Liège, Gembloux 5030, Belgium*

Xin Li − *Institute of Food Science and Technology, Chinese Academy of Agricultural Sciences/Key Laboratory of Agro-Products Quality & Safety in Harvest, Storage, Transportation, Management and Control, Ministry of*

https://doi.org/10.1021/acs.jafc.4c00082
J. Agric. Food Chem. 2024, 72, 11724−11732

Agriculture and Rural Affairs, Beijing 100193, P. R. China; orcid.org/0000-0001-7924-6449

Juan Li − *Institute of Food Science and Technology, Chinese Academy of Agricultural Sciences/Key Laboratory of Agro-Products Quality & Safety in Harvest, Storage, Transportation, Management and Control, Ministry of Agriculture and Rural Affairs, Beijing 100193, P. R. China*

Xiaolan Huang − *Institute of Food Science and Technology, Chinese Academy of Agricultural Sciences/Key Laboratory of Agro-Products Quality & Safety in Harvest, Storage, Transportation, Management and Control, Ministry of Agriculture and Rural Affairs, Beijing 100193, P. R. China*

Yuqiang Bai − *Institute of Food Science and Technology, Chinese Academy of Agricultural Sciences/Key Laboratory of Agro-Products Quality & Safety in Harvest, Storage, Transportation, Management and Control, Ministry of Agriculture and Rural Affairs, Beijing 100193, P. R. China*

Martine Schroyen − *Precision Livestock and Nutrition Unit, Gembloux Agro-Bio Tech, University of Liège, Gembloux 5030, Belgium*

Chengli Hou − *Institute of Food Science and Technology, Chinese Academy of Agricultural Sciences/Key Laboratory of Agro-Products Quality & Safety in Harvest, Storage, Transportation, Management and Control, Ministry of Agriculture and Rural Affairs, Beijing 100193, P. R. China*

Zhenyu Wang − *Institute of Food Science and Technology, Chinese Academy of Agricultural Sciences/Key Laboratory of Agro-Products Quality & Safety in Harvest, Storage, Transportation, Management and Control, Ministry of Agriculture and Rural Affairs, Beijing 100193, P. R. China*

Complete contact information is available at: https://pubs.acs.org/10.1021/acs.jafc.4c00082

Funding

This study was financially supported by the Key Program from the National Natural Science Foundation of China (32030086) in China.

Notes

The authors declare no competing financial interest.

REFERENCES

(1) Schwägele, F.; Haschke, C.; Krauss, G.; Honikel, K. O. Comparative studies of pyruvate kinase from PSE and normal pig muscles. *Z. Lebensm.-Unters. Forsch.* **1996**, *203* (1), 14−20.

(2) Huang, C. Y.; Zhang, D. Q.; Blecker, C.; Zhao, Y. X.; Xiang, C.; Wang, Z. Y.; Li, S. B.; Chen, L. Effects of phosphoglycerate kinase 1 and pyruvate kinase M2 on metabolism and physiochemical changes in postmortem muscle. *Food Chem.: X* **2024**, *21*, 101125.

(3) Yang, B.; Liu, X. Application of proteomics to understand the molecular mechanisms determining meat quality of beef muscles during postmortem aging. *PLoS One* **2021**, *16* (3), 0246955.

(4) Huang, C.; Zhang, D.; Wang, Z.; Zhao, Y.; Blecker, C.; Li, S.; Zheng, X.; Chen, L. Validation of protein biological markers of lamb meat quality characteristics based on the different muscle types. *Food Chem.* **2023**, *427*, 136739.

(5) Gagaoua, M.; Hughes, J.; Terlouw, E. C.; Warner, R. D.; Purslow, P. P.; Lorenzo, J. M.; Picard, B. Proteomic biomarkers of beef colour. *Trends Food Sci. Technol.* **2020**, *101*, 234−252.

(6) Te Pas, M. F.; Kruijt, L.; Pierzchala, M.; Crump, R. E.; Boeren, S.; Keuning, E.; Hoving-Bolink, R.; Hortos, M.; Gispert, M.; Arnau, J.; et al. Identification of proteomic biomarkers in M. Longissimus dorsi as potential predictors of pork quality. *Meat Sci.* **2013**, *95* (3), 679−687.

(7) Gao, X.; Wang, H.; Yang, J. J.; Liu, X.; Liu, Z. R. Pyruvate kinase M2 regulates gene transcription by acting as a protein kinase. *Mol. Cell* **2012**, *45*, 598−609.

(8) Gomord, V.; Faye, L. Posttranslational modification of therapeutic proteins in plants. *Curr. Opin. Plant Biol.* **2004**, *7* (2), 171−181.

(9) Lv, L.; Xu, Y. P.; Zhao, D.; Li, F. L.; Wang, W.; Sasaki, N. Y.; Jiang, Y.; Zhou, X.; Li, T. T.; Guan, K. L.; et al. Mitogenic and oncogenic stimulation of K433 acetylation promotes PKM2 protein kinase activity and nuclear localization. *Mol. Cell* **2013**, *52* (3), 340−352.

(10) Hitosugi, T.; Kang, S.; Vander Heiden, M. G.; Chung, T. W.; Elf, S.; Lythgoe, K.; Dong, S.; Lonial, S.; Wang, X.; Chen, G. Z.; et al. Tyrosine phosphorylation inhibits PKM2 to promote the Warburg effect and tumor growth. *Sci. Signal.* **2009**, *2* (97), ra73.

(11) Li, X.; Zhang, D.; Ren, C.; Bai, Y.; Ijaz, M.; Hou, C.; Chen, L. Effects of protein posttranslational modifications on meat quality: a review. *Compr. Rev. Food Sci. Food Saf.* **2021**, *20* (1), 289−331.

(12) Chen, L.; Li, Z.; Everaert, N.; Lametsch, R.; Zhang, D. Quantitative phosphoproteomic analysis of ovine muscle with different postmortem glycolytic rates. *Food Chem.* **2019**, *280*, 203−209.

(13) Li, Z.; Li, M.; Li, X.; Xin, J.; Wang, Y.; Shen, Q. W.; Zhang, D. Quantitative phosphoproteomic analysis among muscles of different color stability using tandem mass tag labeling. *Food Chem.* **2018**, *249*, 8−15.

(14) Jiang, S.; Liu, Y.; Shen, Z.; Zhou, B.; Shen, Q. W. Acetylome profiling reveals extensive involvement of lysine acetylation in the conversion of muscle to meat. *J. Proteonomics* **2019**, *205*, 103412.

(15) Nandi, S.; Razzaghi, M.; Srivastava, D.; Dey, M. Structural basis for allosteric regulation of pyruvate kinase M2 by phosphorylation and acetylation. *J. Biol. Chem.* **2020**, *295* (51), 17425−17440.

(16) Ren, C.; Song, X. B.; Dong, Y.; Hou, C. L.; Chen, L.; Wang, Z. Y.; Li, X.; Schroyen, M.; Zhang, D. Q. Protein phosphorylation induced by pyruvate kinase M2 inhibited myofibrillar protein degradation in post-mortem muscle. *J. Agric. Food Chem.* **2023**, *71* (41), 15280−15286.

(17) Li, K.; Fu, L. J.; Zhao, Y. Y.; Xue, S. W.; Wang, P.; Xu, X. L.; Bai, Y. H. Use of high-intensity ultrasound to improve emulsifying properties of chicken myofibrillar protein and enhance the rheological properties and stability of the emulsion. *Food Hydrocolloids* **2020**, *98*, 105275.

(18) Guerrero-Mendiola, C.; Oria-Hernandez, J.; Ramirez-Silva, L. Kinetics of the thermal inactivation and aggregate formation of rabbit muscle pyruvate kinase in the presence of trehalose. *Arch. Biochem. Biophys.* **2009**, *490* (2), 129−136.

(19) Kim, S. C.; Sprung, R.; Chen, Y.; Xu, Y. D.; Ball, H.; Pei, J.; Cheng, T.; Kho, Y.; Xiao, H.; Xiao, L.; Grishin, N. V.; White, M.; Yang, X. J.; Zhao, Y. M. Substrate and functional diversity of lysine acetylation revealed by a proteomics survey. *Mol. Cell* **2006**, *23* (4), 607−618.

(20) Niu, H.; Wan, L.; Busygina, V.; Kwon, Y.; Allen, J. A.; Li, X.; Kunz, R. C.; Kubota, K.; Wang, B.; Sung, P.; Shokat, K. M.; Gygi, S. P.; Hollingsworth, N. M. Regulation of meiotic recombination via Mek1-mediated Rad54 phosphorylation. *Mol. Cell* **2009**, *36* (3), 393−404.

(21) Wei, Y.; Zou, Z.; Becker, N.; Anderson, M.; Sumpter, R.; Xiao, G.; Kinch, L.; Koduru, P.; Christudass, C. S.; Veltri, R. W.; Grishin, N. V.; Peyton, M.; Minna, J.; Bhagat, G.; Levine, B. Egfr-mediated beclin 1 phosphorylation in autophagy suppression, tumor progression, and tumor chemoresistance. *Cell* **2013**, *154* (6), 1269−1284.

(22) Maskevich, A. A.; Stsiapura, V. I.; Kuzmitsky, V. A.; Kuznetsova, I. M.; Povarova, O. I.; Uversky, V. N.; Turoverov, K. K. Spectral properties of thioflavin T in solvents with different dielectric properties and in a fibril-incorporated form. *J. Proteome Res.* **2007**, *6*, 1392−1401.

(23) Shen, L.; Gan, M.; Chen, L.; Zhao, Y.; Niu, L.; Tang, G.; Jiang, Y.; Zhang, T.; Zhang, S.; Zhu, L. miR-152 targets pyruvate kinase to

regulate the glycolytic activity of pig skeletal muscles and affects pork quality. *Meat Sci.* **2022**, *185*, 108707.
(24) Chen, X.; Chen, S.; Yu, D. Protein kinase function of pyruvate kinase M2 and cancer. *Cancer Cell Int.* **2020**, *20* (1), 523.
(25) Lu, Z. M.; Hunter, T. Metabolic kinases moonlighting as protein kinases. *Trends Biochem. Sci.* **2018**, *43* (4), 301−310.
(26) He, C. L.; Bian, Y. Y.; Xue, Y.; Liu, Z. X.; Zhou, K. Q.; Yao, C. F.; Lin, Y.; Zou, H. F.; Luo, F. X.; Qu, Y. Y.; Zhao, J. Y.; Ye, M. L.; Zhao, S. M.; Xu, W. Pyruvate kinase M2 activates mTORC1 by phosphorylating AKT1S1. *Sci. Rep.* **2016**, *6*, 21524.
(27) Jin, Z. H.; Wei, Z. H. Molecular simulation for food protein-ligand interactions: A comprehensive review on principles, current applications, and emerging trends. *Compr. Rev. Food Sci. Food Saf.* **2024**, *23*, 13208.
(28) Lv, L.; Li, D.; Zhao, D.; Lin, R. T.; Chu, Y. J.; Zhang, H.; Zha, Z. Y.; Liu, Y.; Li, Z.; Xu, Y. P.; Wang, G.; Huang, Y. R.; Xiong, Y.; Guan, K. L.; Lei, Q. Y. Acetylation targets the M2 isoform of pyruvate kinase for degradation through chaperone-mediated autophagy and promotes tumor growth. *Mol. Cell* **2011**, *42* (6), 719−730.
(29) Larsen, T. M.; Benning, M. M.; Wesenberg, G. E.; Rayment, I.; Reed, G. H. Ligand-Induced Domain Movement in Pyruvate Kinase: Structure of the Enzyme from Rabbit Muscle with Mg2+, K+, andl-Phospholactate at 2.7 Å Resolution. *Arch. Biochem. Biophys.* **1997**, *345* (2), 199−206.
(30) Li, F.; Yu, T.; Zhao, Y.; Yu, S. Probing the catalytic allosteric mechanism of rabbit muscle pyruvate kinase by tryptophan fluorescence quenching. *Eur. Biophys. J.* **2012**, *41* (7), 607−614.
(31) Dang, C. V. PKM2 tyrosine phosphorylation and glutamine metabolism signal a different view of the Warburg effect. *Sci. Signal.* **2009**, *2* (97), 75.
(32) Liang, L. J.; Yang, F. Y.; Wang, D.; Zhang, Y. F.; Yu, H.; Wang, Z.; Sun, B. B.; Liu, Y. T.; Wang, G. Z.; Zhou, G. B. CIP2A induces PKM2 tetramer formation and oxidative phosphorylation in non-small cell lung cancer. *Cell Discovery* **2024**, *10*, 13.
(33) Moore, B. Bifunctional and moonlighting enzymes: lighting the way to regulatory control. *Trends Plant Sci.* **2004**, *9* (5), 221−228.
(34) Park, S. H.; Ozden, O.; Liu, G. X.; Song, H. Y.; Zhu, Y. M.; Yan, Y. F.; Zou, X. H.; Kang, H. J.; Jiang, H. Y.; Principe, D. R.; et al. SIRT2-mediated deacetylation and tetramerization of pyruvate kinase directs glycolysis and tumor growth. *Cancer Res.* **2016**, *76* (13), 3802−3812.
(35) Apostolidi, M.; Vathiotis, I. A.; Muthusamy, V.; Gaule, P.; Gassaway, B. M.; Rimm, D. L.; Rinehart, J. Targeting pyruvate kinase M2 phosphorylation reverses aggressive cancer phenotypes. *Cancer Res.* **2021**, *81* (16), 4346−4359.
(36) Liang, J.; Cao, R. X.; Wang, X. J.; Zhang, Y. J.; Wang, P.; Gao, H.; Li, C.; Yang, F.; Zeng, R.; Wei, P.; et al. Mitochondrial PKM2 regulates oxidative stress-induced apoptosis by stabilizing Bcl2. *Cell Research* **2017**, *27* (3), 329−351.
(37) Wooll, J. O.; Friesen, R. H.; White, M. A.; Watowich, S. J.; Fox, R. O.; Lee, J. C.; Czerwinski, E. W. Structural and functional linkages between subunit interfaces in mammalian pyruvate kinase. *J. Mol. Biol.* **2001**, *312* (3), 525−540.

https://doi.org/10.1021/acs.jafc.4c00082
J. Agric. Food Chem. 2024, 72, 11724−11732